

# fKAN: Fractional Kolmogorov-Arnold Networks with trainable Jacobi basis functions

Alireza Afzal Aghaei<sup>1</sup>

Independent Researcher  
alirezaafzalaghaei@gmail.com

**Abstract.** Recent advancements in neural network design have given rise to the development of Kolmogorov-Arnold Networks (KANs), which enhance speed, interpretability, and precision. This paper presents the Fractional Kolmogorov-Arnold Network (fKAN), a novel neural network architecture that incorporates the distinctive attributes of KANs with a trainable adaptive fractional-orthogonal Jacobi function as its basis function. By leveraging the unique mathematical properties of fractional Jacobi functions, including simple derivative formulas, non-polynomial behavior, and activity for both positive and negative input values, this approach ensures efficient learning and enhanced accuracy. The proposed architecture is evaluated across a range of tasks in deep learning and physics-informed deep learning. Precision is tested on synthetic regression data, image classification, image denoising, and sentiment analysis. Additionally, the performance is measured on various differential equations, including ordinary, partial, and fractional delay differential equations. The results demonstrate that integrating fractional Jacobi functions into KANs significantly improves training speed and performance across diverse fields and applications.

**Keywords:** Activation Functions, Jacobi Polynomials, Kolmogorov-Arnold Networks, Physics-informed Deep Learning

## 1 Introduction

The activation function in artificial neural networks is a mathematical construct that parallels the biological concept of an action potential, which determines neuronal activity. Essentially, the activation function applies a mathematical operation to the raw output of neurons within an artificial neural network, producing the final output. The value derived from this activation process is then transmitted to other neurons in the network, emphasizing the significant influence the choice of activation function has on network performance. Over time, various activation functions have been introduced in the literature [2, 39], prompting extensive research to understand and evaluate their impact on network dynamics.

The Sigmoid function, a notable non-linear activation function, has been extensively studied for its efficacy in artificial neural networks [34]. This function is characterized by its differentiability, a feature that aids in weight updates during the backpropagation algorithm, as its derivative is inherently based on the function itself. However, it has unintended side effects, such as the vanishing gradient problem within the network. This has led researchers to propose enhanced versions of the sigmoid function, as explored in [72]. The hyperbolic tangent function, another well-known activation function, shares similar drawbacks, intensifying challenges like the vanishing gradient problem in neural networks [46].

In 2010, Nair and Hinton introduced a revolutionary activation function known as the Rectified Linear Unit (ReLU), which has since become the most commonly used activation function in recent years [59]. Numerous studies have investigated the impact of ReLU on the learning process within neural networks, with significant contributions from researchers like Glorot et al. [29] and Ramachandran et al. [74]. ReLU, a non-linear activation function, provides differentiability and a derivative formula based on the function itself. However, it has a limitation in that it returns 0 for negative inputs, leading to ‘dead neurons’ in the network, which obstructs the acquisition of meaningful knowledge. To address this issue, researchers have proposed improved versions of ReLU, including Leaky ReLU [54], Parametric ReLU [35], Gaussian Error Linear Units (GELU) [36], Exponential Linear Units (ELU) [16], and Mish [58].

Building on the foundation laid by ReLU and its variants, the concept of trainable or adaptive activation functions has emerged as a promising avenue in neural network research. These functions, unlike their fixed

counterparts, can adjust their behavior based on the data they process, potentially leading to more efficient and effective learning processes. Adaptive activation functions, such as the Parametric ReLU introduced by He et al. [35], the Learnable Extended Activation Function proposed by Bodyanskiy et al. [10], modReLU developed by Arjovsky et al. [5], and DELU explored by Pishchik [70], allow the parameters of the activation function to be learned during the training process, adapting to the specific characteristics of the input data. This adaptability can mitigate some of the inherent limitations of fixed activation functions, such as the 'dead neuron' problem associated with ReLU, by ensuring that the activation function evolves in tandem with the network's learning trajectory. The exploration of such functions is driven by the hypothesis that a network's capacity to learn can be significantly improved by allowing more aspects of the model, including the activation function, to be subject to optimization.

In recent developments, the emergence of Kolmogorov-Arnold Neural Networks has been noted [50]. These networks represent an innovative category within neural network architectures, utilizing the mathematical characteristics of splines and B-splines activation functions to achieve precise data approximation. Inspired by the Kolmogorov-Arnold representation theorem, KANs replace traditional linear weights with trainable 1D functions parametrized as splines. This substitution allows KANs to capture complex patterns without the need for linear weights, leading to a more flexible and interpretable model. The structure of KANs offers several advantages over conventional Multi-Layer Perceptrons (MLPs).

These networks can achieve comparable or superior accuracy in tasks such as data fitting and solving partial differential equations with significantly smaller network sizes [50, 15, 49]. Moreover, the use of splines as activation functions on edges enhances the interpretability of the network, making it easier to visualize and understand the decision-making process [50]. Empirical studies have also shown that KANs exhibit faster neural scaling laws than MLPs, suggesting that they can scale more efficiently with increasing data size [50, 26, 1].

The field of KANs has seen significant advancements since the introduction of the KAN architecture by the B-splines. This architecture has paved the way for the development of various types of KANs, each with its unique features and applications. One such extension is the Wavelet KANs [11], introduced by Bozorgasl and his team. This innovative approach incorporates orthogonal Wavelets into the KAN architecture. The integration of Wavelets has been instrumental in enhancing the performance of KANs, while also improving their interpretability. Another noteworthy development in the field is the Fourier KANs [92] by Xu and colleagues. This model was specifically designed for efficient graph-based recommendation systems within a graph collaborative filtering framework. The Fourier KANs have proven to be highly effective in making accurate recommendations, thereby enhancing the user experience on various digital platforms. Similarly, Genet et al. introduced Temporal KANs, a recurrent neural network architecture inspired by Long Short Term Memory (LSTM) networks, as outlined in [27]. Temporal KANs excel in handling sequential data tasks like time-series analysis and natural language processing, capitalizing on the strengths of LSTM networks. Another notable advancement in the context of KANs is the development of deep operator networks for mechanical problems, discussed in [1]. Additionally, Samadi et al. conducted a comprehensive analysis of KANs, focusing on their smoothness properties, in their work on smooth KANs [76].

In numerical analysis [80, 25, 79], different basis functions have been utilized to approximate functions. Splines, Fourier basis, rational functions, Wavelets, Binary-valued functions, and polynomials are some of the most common options. Fourier functions are one of the best choices for problems with periodic oscillations. Splines, despite their inherent intricacies, are great options for approximating complex shapes because of their flexibility. These intricacies include piece-wise nature, continuity issues, and complex implementation. On the other hand, polynomials are an alternative option when it comes to approximating functions. Polynomials offer simpler implementation, continuity, and global adaptation. However, they suffer of Runge's phenomenon, numerical instability, and even overfitting. Moreover, the nature of these basis functions does not allow for an accurate approximation of an unknown function with a low degree.

Orthogonal polynomials are a set of polynomials introduced to mitigate the limitations of raw polynomials. These functions build a complete set of basis functions and have the orthogonality property, which ensures that each pair of functions in the set is perpendicular to each other [79]. This property ensures various mathematical theorems and corollaries that mitigate problems such as Runge's phenomenon. Among the emerging trends in the field of neural network activation functions, the use of orthogonal polynomials has attracted significant attention in the literature. For example, Deepthi et al. [17] developed the Chebyshev activation function for classification and image denoising, Alsaadi et al. [3] developed a Chebyshev neural network to control a hydraulic generator regulating system, Venkatappareddy et al. [88] modeled the max pooling layer with Legendre polynomials, Wang et al. [90] developed a hybrid neural network based on Laguerre polynomials for wind power forecasting, Patra et al. [66] utilized Laguerre neural networks for wireless sensor networks, Ebrahimi et al. [21] classified ECG signals based on Hermite functions and neural networks, Guo et al. [31] used Bernstein polynomials in graph neural

networks. Additionally, Sidharth [82] introduced Chebyshev KANs, showcasing another innovative application of polynomial-based neural network architectures.

All attempts and explorations to find an optimal activation function, possibly piece-wise, rely on certain mathematical functions that appear to be a good fit for some physical or engineering problems. However, most of these functions, especially orthogonal polynomials, are interconnected. In fact, all these functions are subsets of the well-known Generalized hypergeometric function [13, 79, 23, 56]. This parametric function can be reduced to any of the aforementioned orthogonal activation functions and yield the same results. To illustrate these relationships more clearly, we have plotted them in Figure 1 which also depicts a literature review of neural network activation functions. Based on the hierarchy depicted in this figure, one can obtain Chebyshev polynomials by fixing parameters of the Gegenbauer, Jacobi, or hypergeometric function.

As observed, the majority of research papers concentrate on specific instances of the hypergeometric function. This can be directly attributed to the unique properties of these functions. For instance, Legendre polynomials possess a simple orthogonality property that can expedite certain calculations, while Chebyshev polynomials have theoretical foundations that make them the most accurate function approximations. Laguerre and Hermite polynomials can manage input values beyond a finite domain, a prerequisite for Chebyshev and Legendre polynomials. Additionally, the rapid computation of these functions' derivatives is another property that needs consideration. Specifically, the leaves in Figure 1 are very special functions with numerous mathematical properties, while nodes near the root have fewer mathematical properties but more general definitions.

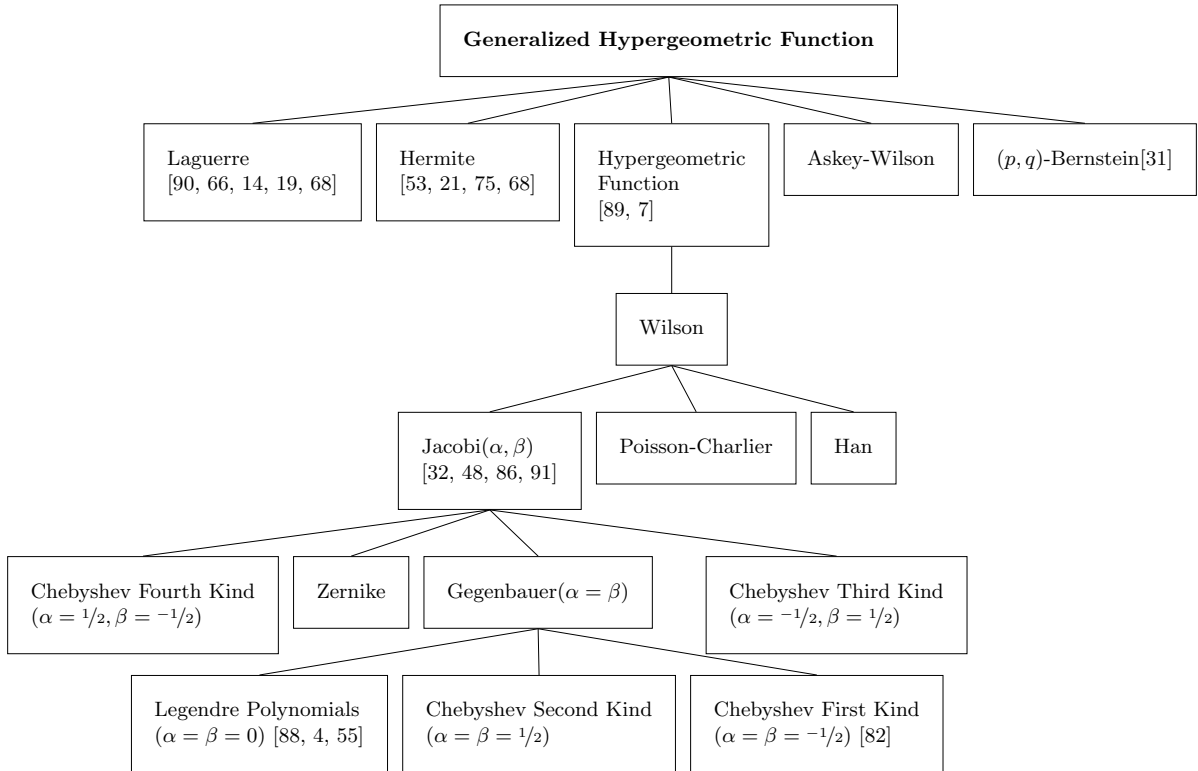


Fig. 1: This figure depicts the hierarchical classification of the generalized hypergeometric function. It shows that Chebyshev and Gegenbauer polynomials are particular cases within the more general class of Jacobi polynomials, which itself is a subclass of the hypergeometric function.

Regardless of these interesting properties, orthogonal polynomials are still polynomials and inherit the limitations of polynomials. Fractional orthogonal functions are an extension of orthogonal polynomials that map their functional space from polynomials to fractional functions [73]. These functions are commonly used in numerical analysis and simulating differential equations [62, 63]. However, in some cases, they have been used in neural

networks [33]. This mapping has been developed for various functions including B-splines and Wavelets [87, 9], Bernoulli functions [61], Jacobi functions [64], Legendre polynomials [65], and Lagrange functions [18]. The results of these approximations consistently indicate that introducing a fractional order parameter to the basis functions leads to more accurate predictions, even when the fractional order parameter itself is to be determined.

In this paper, we focus on a well-known orthogonal polynomial in the middle of the tree (Figure 1), the Jacobi polynomial, to propose a new trainable activation function for KANs. We demonstrate how the parameters of Jacobi polynomials, shaping the activation function, can be tuned during the training process to enhance neural network performance. Additionally, we explore how the fractional order of the Jacobi functions can be leveraged to further increase the accuracy of the network. While the Jacobi polynomial has been utilized in various neural network architectures by researchers such as Tao et al. [86] and Wang et al. [91], who employed these functions in Graph neural networks, or Hadian et al. [32] and Liu et al. [48], who employed these functions in physics-informed neural network architectures for the solution of differential equations, this paper aims to provide a novel perspective on orthogonal Jacobi functions. We introduce a fractional Jacobi neural block that can be integrated anywhere in a deep or KAN architecture.

To be more specific, we delve into the effectiveness of fractional Jacobi functions as activation functions, comparing them to common alternatives in neural networks. Subsequently, a novel neural network block is introduced, enabling the use of the proposed activation function in different neural network architectures. Then, we assess the accuracy of the presented method in different deep learning benchmark tasks. We will employ this neural architecture for approximating synthetic regression data, then we use it to classify the MNIST digit classification dataset, denoise the Fashion MNIST dataset, and finally conduct a sentiment analysis task on the IMDB dataset. To further evaluate the proposed neural network, we employ it to approximate the solution of some differential equations. We examine the standard form of the Lane-Emden equation, the one-dimensional Burgers partial differential equation, and a delay differential equation with the Caputo fractional derivative.

The following sections of the paper are structured as follows. First, we explain activation functions and their impact on MLPs and KANs. Then, we explore the characteristics of Jacobi polynomials, highlighting their intrinsic properties. In this section, we discuss the advantages that make Jacobi polynomials well-suited as activation functions in neural networks. Next, we present the methodology proposed in this research by detailing the development of a fKAN. Section 4 validates the proposed method through experiments on real-world problems. Finally, the concluding section offers some final remarks.

## 2 Background

In this section, we provide an overview of MLPs and KANs, focusing on the role of activation functions within these networks. We then explore the key characteristics that define an effective activation function. Following this, we discuss Jacobi polynomials and their relationship to other orthogonal functions, highlighting their suitability for neural networks.

### 2.1 Multi-Layer Perceptron

A Multi-Layer Perceptron, grounded in the universal approximation theory [69, 60, 43], aims to find a weighted summation of various basis functions. Specifically, an approximation to function  $\chi(\cdot)$  can be done using:

$$\chi(\zeta) \approx \hat{\chi}(\zeta) = \sigma \left( b + \sum_{q=0}^Q \theta_q \zeta_q \right).$$

The universal approximation theory states that a network with a single hidden layer containing a finite number of neurons, can approximate continuous functions on compact subsets of  $\mathbb{R}^d$ , under mild assumptions on the activation function  $\sigma(\cdot)$ . In a mathematical sense, it ensures that exists some  $\theta$  and  $b$  such that:

$$\sup_{\zeta \in \mathbb{R}^d} \|\chi(\zeta) - \hat{\chi}(\zeta)\| < \epsilon.$$

In practice, the accuracy of this estimation improves as a result of the non-linear nested composition of these approximations [30, 52, 41]. Mathematically, an MLP can be represented as:

$$\begin{aligned} \mathcal{H}_0 &= \zeta, & \zeta &\in \mathbb{R}^d, \\ \mathcal{H}_i &= \sigma_i(\theta^{(i)} \mathcal{H}_{i-1} + b^{(i)}), & i &= 1, 2, \dots, L-1, \\ \mathcal{H}_L &= \psi(\theta^{(L)} \mathcal{H}_{L-1} + b^{(L)}). \end{aligned}$$

In this definition,  $\zeta$  represents the input sample fed into the input layer  $\mathcal{H}_0$ . The output of the  $i$ -th layer,  $\mathcal{H}_i$ , is computed based on the output of the previous layer,  $\mathcal{H}_{i-1}$ . This computation involves matrix multiplication between the learnable weights  $\theta^{(i)}$  and the output of the previous layer,  $\mathcal{H}_{i-1}$ . This weight matrix can be either dense or possess a special structure, such as a Toeplitz matrix, which is commonly used in convolutional neural networks (CNNs). Additionally, a bias term  $b^{(i)}$  is added to this result to shift the activation function and better fit the data. In this scenario, a non-linear activation function  $\sigma_i(\cdot)$  is applied to the result to overcome the limitations of linear combinations and capture more complex patterns within the data. The output layer of the network,  $\mathcal{H}_L$ , is computed using a final activation function, which is typically a linear function for regression tasks and a Sigmoid or softmax function for classification tasks.

Following the forward pass, the neural network's overall error on the training data is computed. During the backpropagation phase, the gradients of the error with respect to each weight are calculated and used to update the weights, thereby minimizing the error. In this phase, the derivative of the activation function plays a crucial role, as it is used to adjust the network weights in a manner that reduces the overall network error. Therefore, one of the most significant properties of an activation function is its differentiability. According to [39], an effective activation function should possess the following properties:

- Differentiability: During the optimization process, the ability to compute the activation function's derivative is vital. Differentiability ensures the smooth updating of weights; without it, the process is disrupted.
- Non-linearity: Activation functions generally fall into two categories - linear and non-linear. Networks with multiple layers of linear or identical activation functions behave similarly to single-layer networks with the same characteristics. Therefore, non-linear activation functions are particularly valuable, as they enable the network to extract complex information from data, enhancing the network's capacity for learning.
- Finite Range/Boundedness: Since the activation function determines a neuron's final output, limiting the output values to a specific interval enhances network stability.
- Vanishing and Exploding Gradient Issues: In the backpropagation process, the chain rule is employed to adjust weights. In essence, the gradients in the initial layers are derived from the product of gradients in the final layers. If these generated gradients become exceedingly small or excessively large, the challenges of gradient vanishing or exploding arise, hindering the correct weight updates in the initial layers.
- Computational Efficiency: The activation function's formulation should be structured to ensure that both the forward and backward processes in the network do not involve intricate or resource-intensive computations.

## 2.2 Kolmogorov-Arnold Networks

In contrast to MLPs, KANs are based on the Kolmogorov-Arnold representation theorem, which states that a multivariate continuous function can be expressed as a finite composition of continuous functions of a single variable and the binary operation of addition [12, 42]. Mathematically:

$$\chi(\zeta) \approx \hat{\chi}(\zeta) = \sum_{q=0}^{2d} \Phi_q \left( \sum_{p=1}^d \phi_{q,p}(\zeta_p) \right),$$

for some  $d$  with trainable functions  $\Phi_q : \mathbb{R} \rightarrow \mathbb{R}$ ,  $\phi_{q,p} : [0, 1] \rightarrow \mathbb{R}$  and known function  $\chi(\zeta) : [0, 1]^d \rightarrow \mathbb{R}$ . As proposed by the KAN [50], one may consider B-spline [23, 56] curves combined with the SiLU activation function [67] for these functions. Regardless of the choices of these functions, in matrix form, we can formulate the KANs as:

$$\hat{\chi}(\zeta) = \Phi_{n-1} \circ \dots \circ \Phi_1 \circ \Phi_0 \circ \zeta,$$

where  $\Phi_{p,q} = \phi_{p,q}(\cdot)$ . The convergence of this approximation can be seen as:

$$\max_{|\alpha| \leq m} \sup_{\zeta \in [0,1]^d} \|\mathfrak{D}^\alpha \{\chi(\zeta) - \hat{\chi}(\zeta)\}\| < \epsilon,$$

where  $\mathfrak{D}$  is the derivative operator, and  $\epsilon$  is a constant based on the behavior of  $\chi(\cdot)$  and trainable functions  $\phi_{p,q}(\cdot)$ . The complete proof of the convergence of this approximation can be found in [50, 12, 20, 77].

As a consequence of this theorem and its utility, various extensions have been proposed to facilitate faster implementations. For example, Lorentz [51] proved that the functions  $\Phi_q(\cdot)$  can be reduced to a single function  $\Phi(\cdot)$ :

$$\hat{\chi}(\zeta) = \sum_{q=0}^{2d} \Phi \left( \sum_{p=1}^d \phi_{q,p}(\zeta_p) \right).$$

In another work, Sprecher [81] showed that the functions  $\phi_{p,q}$  can be replaced by a single function  $\phi(\cdot)$ :

$$\hat{\chi}(\zeta) = \sum_{q=0}^{2d} \Phi \left( q + \sum_{p=1}^d \theta_p \phi(\zeta_p + \nu q) \right).$$

Both of these variants aimed to provide an easier approach for implementation. However, they have not yet addressed the issues of the Kolmogorov-Arnold representation, which include the non-smoothness of the inner functions and the time complexity of KANs [28].

Recently, some research has proposed replacements for B-splines and alternative formulations of KANs to potentially achieve more accurate solutions with lower time complexity. For example, Fourier KANs [92], Wavelet KANs [11], and radial basis function (RBF) KANs [47]. Another approach is Chebyshev KANs, which utilize orthogonal polynomials as the univariate functions in KANs [82, 83]. This architecture is defined as:

$$\hat{\chi}(\zeta) = \sum_{q=1}^n \sum_{p=1}^d \theta_{p,q} T_q(\tanh(\zeta_p)).$$

Here,  $n$ , a hyperparameter, represents the degree of the Chebyshev polynomials,  $T_q(\cdot)$  denotes the Chebyshev polynomial of degree  $q$ , and  $\theta_{p,q}$  are the trainable weights. This approach is a counterpart of KANs, named Learnable Activation Networks (LANs).

Although the Chebyshev KAN demonstrated acceptable accuracy while maintaining low computational complexity [82, 83], it still inherits the limitations associated with polynomials as discussed in the introduction. In the following section, we introduce fractional Jacobi functions as a potential replacement for Chebyshev polynomials in KANs.

### 2.3 Jacobi polynomials

The Jacobi polynomials  $\mathcal{J}_n^{(\alpha,\beta)}(\zeta)$  are a special case of hypergeometric functions. The generalized form of the hypergeometric function  ${}_p\mathcal{F}_q : \mathbb{C}^{p+q+1} \rightarrow \mathbb{C}$  can be represented as:

$${}_p\mathcal{F}_q \left( \begin{matrix} a_1, a_2, \dots, a_p \\ b_1, b_2, \dots, b_q \end{matrix}; \zeta \right) = \sum_{n=0}^{\infty} \frac{(a_1)_n (a_2)_n \dots (a_p)_n \zeta^n}{(b_1)_n (b_2)_n \dots (b_q)_n n!},$$

where  $(a)_n$  is the rising sequential product, known as the Pochhammer symbol, defined by:

$$(a)_n = \frac{\Gamma(a+n)}{\Gamma(a)} = a(a+1)(a+2)\dots(a+n-1), \quad n > 0,$$

in which  $\Gamma(\xi) = \int_0^{\infty} s^{\xi-1} \exp(-s) ds$  is the Gamma function [79]. In the case of  $n = 1$ , this empty product is defined as one [7]. Vieira [89] proved that the infinite hypergeometric series converges if any of the following conditions are met:

- (a)  $p \leq q$ ,
- (b)  $q = p - 1 \wedge |\zeta| < 1$ ,
- (c)  $q = p - 1 \wedge \Re \left( \sum_{i=1}^{p-1} (b_i - p) - \sum_{j=1}^q a_j \right) > 0 \wedge |\zeta| = 1$ .

For  $p = 2$  and  $q = 1$ , this analytic function simplifies to the Gaussian hypergeometric function:

$${}_2\mathcal{F}_1 \left( \begin{matrix} a_1, a_2 \\ b_1 \end{matrix}; \zeta \right) = \sum_{n=0}^{\infty} \frac{(a_1)_n (a_2)_n \zeta^n}{(b_1)_n n!}.$$

Similarly, for  $p = 0$  and  $q = 1$ , the generalized hypergeometric function transforms into the Bessel function:

$$J_{\alpha}(\zeta) = \frac{\left(\frac{\zeta}{2}\right)^{\alpha}}{\Gamma(\alpha+1)} {}_0\mathcal{F}_1 \left( \alpha+1; -\frac{\zeta^2}{4} \right).$$

The analytical function  ${}_p\mathcal{F}_q$  with any non-positive values of  $a_i$  reduces to a polynomial of degree  $-a_i$  in the argument  $\zeta$ . For example, Askey–Wilson polynomials, Wilson polynomials, continuous Hahn polynomials, and Jacobi polynomials are some such cases.

For the specific choice  $p = 2, q = 1, a_1 = -n, a_2 = n + 1 + \alpha + \beta$ , and  $b_1 = 1 + \alpha$  where  $\alpha, \beta > -1$ , the Gaussian hypergeometric series reduces to the Jacobi polynomials:

$$\mathcal{J}_n^{(\alpha, \beta)}(\zeta) = \frac{(\alpha + 1)_n}{n!} {}_2\mathcal{F}_1 \left( \begin{matrix} -n, n + 1 + \alpha + \beta \\ 1 + \alpha \end{matrix}; \frac{1}{2}(1 - \zeta) \right).$$

These polynomials appear in various scientific fields such as signal processing, numerical analysis, machine learning, economics, and quantum mechanics [73]. Hence, they can be defined through several definitions. For example, they are the eigenfunctions of  $\mathcal{L}(\mathcal{J}_n^{(\alpha, \beta)}) = \lambda_n \mathcal{J}_n^{(\alpha, \beta)}$  for the linear second-order Sturm–Liouville differential operator:

$$\begin{aligned} \mathcal{L}(\mathcal{J}_n^{(\alpha, \beta)}) &:= - (1 - \zeta)^{-\alpha} (1 + \zeta)^{-\beta} \frac{d}{d\zeta} \left( (1 - \zeta)^{\alpha+1} (1 + \zeta)^{\beta+1} \frac{d}{d\zeta} \mathcal{J}_n^{(\alpha, \beta)}(\zeta) \right) \\ &= (\zeta^2 - 1) \frac{d^2}{d\zeta^2} \mathcal{J}_n^{(\alpha, \beta)}(\zeta) + (\alpha - \beta + (\alpha + \beta + 2)\zeta) \frac{d}{d\zeta} \mathcal{J}_n^{(\alpha, \beta)}(\zeta), \end{aligned}$$

with the eigenvalues  $\lambda_n = n(n + 1 + \alpha + \beta)$ . Alternatively, the following three-term recurrence formula can generate the Jacobi polynomials:

$$\begin{aligned} \mathcal{J}_0^{(\alpha, \beta)}(\zeta) &= 1, \\ \mathcal{J}_1^{(\alpha, \beta)}(\zeta) &= A_0\zeta + B_0, \\ \mathcal{J}_{n+1}^{(\alpha, \beta)}(\zeta) &= (A_n\zeta + B_n)\mathcal{J}_n^{(\alpha, \beta)}(\zeta) - C_n\mathcal{J}_{n-1}^{(\alpha, \beta)}(\zeta), \quad n \geq 1, \end{aligned}$$

where

$$\begin{aligned} A_n &= \frac{(2n + \alpha + \beta + 1)(2n + \alpha + \beta + 2)}{2(n + 1)(n + \alpha + \beta + 1)}, \\ B_n &= \frac{(\alpha^2 - \beta^2)(2n + \alpha + \beta + 1)}{2(n + 1)(n + \alpha + \beta + 1)(2n + \alpha + \beta)}, \\ C_n &= \frac{(n + \alpha)(n + \beta)(2n + \alpha + \beta + 2)}{(n + 1)(n + \alpha + \beta + 1)(2n + \alpha + \beta)}. \end{aligned}$$

Choosing different values for  $\alpha$  and  $\beta$  results in specific well-known orthogonal polynomials that appear in different engineering applications. Figure 1 depicts some of the most used functions in this hierarchy. In the following, we focus on the Jacobi polynomials and their properties which are used in the following sections.

**Theorem 1.** *The Jacobi polynomials with  $\alpha, \beta > -1$  are a set of orthogonal functions on the interval  $[-1, 1]$ :*

$$\langle \mathcal{J}_m^{(\alpha, \beta)}, \mathcal{J}_n^{(\alpha, \beta)} \rangle = \int_{-1}^1 \mathcal{J}_m^{(\alpha, \beta)}(\zeta) \mathcal{J}_n^{(\alpha, \beta)}(\zeta) (1 - \zeta)^\alpha (1 + \zeta)^\beta d\zeta = \|\mathcal{J}_n^{(\alpha, \beta)}\|_{2\delta_{m,n}},$$

where  $\langle f, g \rangle = \int_{\Omega} f(\xi)g(\xi)w(\xi)d\xi$  is the inner product operator over the domain  $\Omega \subseteq \mathbb{R}$  [79].

**Theorem 2.** *The Jacobi polynomials have the following symmetry on the interval  $[-1, 1]$  [79]:*

$$\mathcal{J}_n^{(\alpha, \beta)}(-\zeta) = (-1)^n \mathcal{J}_n^{(\beta, \alpha)}(\zeta).$$

**Corollary 1.** *The Jacobi polynomials at the boundary points can be approximated by:*

$$\begin{aligned} \mathcal{J}_n^{(\alpha, \beta)}(-1) &= \frac{(-1)^n}{n!} \frac{\Gamma(n + 1 + \beta)}{\Gamma(1 + \beta)}, \\ \mathcal{J}_n^{(\alpha, \beta)}(+1) &\approx n^\alpha \quad n \gg 1. \end{aligned}$$

**Theorem 3.** *The derivatives of the Jacobi polynomials can be expressed in terms of themselves. Specifically:*

$$\frac{d^m}{d\zeta^m} \mathcal{J}_n^{(\alpha, \beta)}(\zeta) = \frac{\Gamma(n + m + 1 + \alpha + \beta)}{2^m \Gamma(m + 1 + \alpha + \beta)} P_{n-m}^{(\alpha+m, \beta+m)}(\zeta).$$

*Proof.* This property is a direct consequence of the orthogonality and the derivatives of the hypergeometric function:

$$\frac{d^m}{d\zeta^m} {}_2F_1 \left( \begin{matrix} a_1, a_2 \\ b_1 \end{matrix}; \zeta \right) = \frac{(a_1)_m (a_2)_m}{(b_1)_m} {}_2F_1 \left( \begin{matrix} a_1 + m, a_2 + m \\ b_1 + m \end{matrix}; \zeta \right)$$

**Theorem 4.** *Jacobi polynomial of the degree  $n$  has  $n$  real distinct roots [6, 78].*

**Theorem 5.** *The linear bijective mapping*

$$\varphi_{(d_0, d_1)}(\zeta) = \frac{2\zeta - d_0 - d_1}{d_1 - d_0},$$

*transforms the properties of the Jacobi polynomials from the interval  $[-1, 1]$  into the desired domain  $[d_0, d_1]$ . Moreover, for extending the polynomial space into fractional-order functions, one may use:*

$$\varphi_{(d_0, d_1, \gamma)}(\zeta) = \frac{2\zeta^\gamma - d_0 - d_1}{d_1 - d_0}.$$

*Employing these mappings, the shifted fractional Jacobi functions can be generated using:*

$$\mathcal{P}_n^{(\alpha, \beta)}(\zeta) = \mathcal{J}_n^{(\alpha, \beta)}(\varphi_{(d_0, d_1, \gamma)}(\zeta)).$$

Examining the characteristics of Jacobi orthogonal polynomials as a potential activation function reveals their non-linearity and differentiability. Their derivatives can be easily computed using a formula derived from the function itself, simplifying calculations during backpropagation and reducing computational burden. Additionally, Jacobi polynomials inherently confine their output within a predetermined range, promoting network stability. Consequently, they offer promising features for activation functions in neural networks. With these insights, the following section introduces an architecture for incorporating Jacobi functions into neural network frameworks.

### 3 Fractional KAN

In this section, we present a novel block structure enabling the utilization of fractional Jacobi functions as activation functions within a neural network. This framework, empowers deep learning architectures or even KANs to determine optimal values for Jacobi polynomial parameters, namely  $\alpha$ ,  $\beta$ , and the fractional order  $\gamma$ . Following this, we will explore the intricacies of the Jacobi neural block integrated into the design of the neural network models employed in our experiments.

It's crucial to acknowledge that Jacobi polynomials, as per Theorem 1, require their input values to reside within a specific interval to yield meaningful output. However, the output produced by a neural network layer doesn't inherently adhere to this constraint, making it impractical to directly employ Jacobi polynomials as activation functions immediately after a fully connected layer. To tackle this challenge, two different approaches have been proposed: 1) Utilizing batch normalization and 2) Applying a bounded activation function [82].

The first option introduces certain complications, including increased time complexity [24], incompatibility with small batch sizes or online learning [44], and issues with saturating non-linearities [38, 8]. On the other hand, the second approach offers lower computational complexity compared to batch normalization. It facilitates optimal backward computations, boasts easy implementation, and ensures consistent behavior in both the training and testing phases. In contrast, the first option exhibits varying behaviors between these phases. Therefore, in this paper, we opt for the second approach to address this case.

The choice of an activation function to confine the output of a layer within a bounded interval ( $[d_0, d_1]$ ) can include options like the Sigmoid function, hyperbolic tangent, Gaussian function, or any bounded-range activation function. While the selection of this function is arbitrary, in this paper, we opt for the Sigmoid function ( $\sigma(\zeta) = \frac{1}{1 + \exp(-\zeta)}$ ) due to its range, which spans  $(0, 1)$ . This property of positivity enables the computation of fractional powers without encountering complex-valued numbers in fKAN.

To propose the fractional KAN, we first revisit the original KAN:

$$\hat{\chi}(\zeta) = \sum_{q=0}^{2d} \Phi_q \left( \sum_{p=1}^d \phi_{q,p}(\zeta_p) \right).$$

In general, the fractional KAN can be obtained using a fractional univariate function  $\phi_{p,q}(\cdot)$  such as fractional Jacobi functions, fractional Bernoulli functions, or even fractional B-splines [71]. This extension can be formulated as:

$$\hat{\chi}(\zeta) = \sum_{q=0}^{2d} \Phi_q^{(\gamma)} \left( \sum_{p=1}^d \phi_{q,p}^{(\gamma)}(\zeta_p) \right),$$

where  $\gamma$  is the fractional order. In this paper, we choose the fractional Jacobi functions due to their flexibility, ease of calculation, and adaptability. Mathematically, for predefined values of  $\alpha$ ,  $\beta$ , and  $\gamma$ , a basis function can be formulated as:

$$\phi_{p,q}^{(\gamma)}(\zeta_p) = \mathcal{J}_q^{(\alpha,\beta)}(\varphi_{(0,1;\gamma)}(\sigma(\zeta_p))).$$

In order to allow this mathematical function to be tuned for given data during the optimization process of the networks, we can define these predefined parameters to be learned during training. However, this requires some modifications. For example, to ensure that the Jacobi polynomial converges, its parameters  $(\alpha, \beta)$  should be greater than  $-1$ , while a network weight can take any value. To address this, we use the well-known ELU activation function [16] with the  $\text{ELU} : \mathbb{R} \rightarrow (-\kappa, \infty)$  property:

$$\text{ELU}(\zeta; \kappa) = \begin{cases} \zeta & \text{if } \zeta > 0, \\ \kappa \times (e^\zeta - 1) & \text{if } \zeta \leq 0, \end{cases}$$

where  $\kappa$  is a parameter that controls the lower bound of the range of the ELU function. As a result of this definition, for parameters  $\alpha$  and  $\beta$ , one can easily set  $\kappa$  to 1 to obtain meaningful Jacobi functions.

Furthermore, the fractional power  $\gamma$  needs to be positive to ensure the well-definedness of the Jacobi polynomials. For this purpose, one might consider using functions like  $\text{ReLU}(\cdot)$  or  $\text{ELU}(\cdot, 0)$ . However, these functions allow the parameter to approach infinity, potentially causing instability issues such as Runge's phenomenon [79]. Instead, we propose using the Sigmoid function again to constrain the values of  $\gamma$  between zero and one.

This approach, combined with polynomial degrees, enables the network to find an accurate solution for the given data. By fixing the basis function degree to  $n$  (denoted as  $\mathcal{J}_n^{(\alpha,\beta)}(\cdot)$ ), the network can utilize a fractional degree between zero and  $n$ , exhibiting a "liquid" behavior that permits the network to explore the fractional space for approximating the desired function. Putting all of these together, the new basis function for fKAN can be expressed as:

$$\phi_{p,q}^{(\gamma)}(\zeta_p) = \mathcal{J}_q^{(\text{ELU}(\alpha,1), \text{ELU}(\beta,1))}(\varphi_{(0,1;\sigma(\gamma))}(\sigma(\zeta_p))), \quad (1)$$

with trainable parameters  $\alpha$ ,  $\beta$ , and  $\gamma$ . We call this adaptive activation the fractional Jacobi neural block, abbreviated as fJNB. A visualization of the fJNB can be seen in Figure 2.

The next step in defining fKAN is to establish the summation bounds and the function  $\Phi_q(\cdot)$ . In the general definition of KANs, the basis functions  $\phi_{p,q}(\cdot)$  are local functions (e.g., obtained through B-splines or compact support RBFs), meaning they are non-zero only on a subset of the real line. To approximate a desired function, these local functions must be combined with other local functions in that domain. However, in the case of polynomials, especially orthogonal Jacobi polynomials, the function is non-zero except at some root points (see Theorem 4). This allows us to omit the outer summation and focus solely on the inner one. For the function  $\Phi_q(\cdot)$ , now denoted as  $\Phi(\cdot)$ , we can use a simple linear function with trainable weights  $\theta$  that are adjusted during the network's backward phase. This approach is visualized in Figure 3a.

By closely examining the proposed fKAN, one can see that this approach focuses on a specific basis function (e.g.,  $q = 2$ ), which may not be suitable for a wide variety of applications. For example, in numerical analysis, the Taylor series guarantees that a function can be approximated by a linear combination of monomials. As the number of terms in this series tends to infinity, the approximation becomes increasingly accurate. Formally, for some known weights  $\theta_n$ :

$$\chi(\zeta) = \sum_{n=0}^{\infty} \theta_n \zeta^n.$$

To simulate a similar approach in fKANs, we can use the following formulation:

$$\hat{\chi}(\zeta) = \sum_{q=0}^Q \Phi_q^{(\gamma)} \left( \sum_{p=1}^d \phi_{q,p}^{(\gamma)}(\zeta_p) \right).$$

In this formulation,  $Q$  represents the maximum degree of the fKAN and  $\phi_{q,p}^{(\gamma)}(\zeta_p)$  is defined as in equation (1). Notably, the outer summation is independent of the input data. Additionally, the function  $\Phi_q(\cdot)$  can be defined to fuse the outputs of each fJNB using either a concatenation layer or an attention mechanism. This scheme is illustrated in Figure 3b

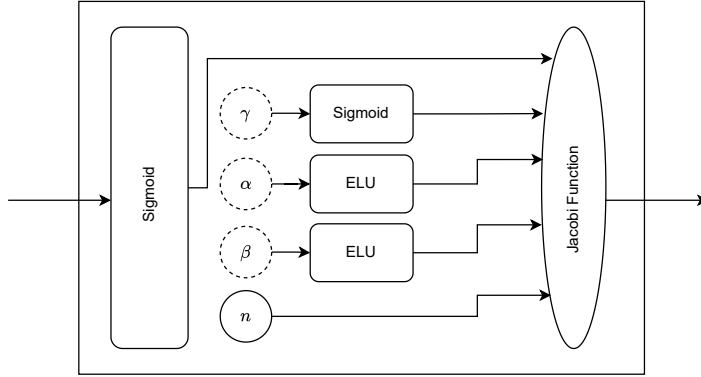


Fig. 2: The architecture of the fractional Jacobi neural block proposed in formula (1), featuring trainable parameters  $\alpha$ ,  $\beta$ , and  $\gamma$ . This block serves as an adaptive activation function, enabling the network to learn optimal values for these parameters during training. The fJNB offers flexibility, ease of calculation, and adaptability, making it suitable for various applications in neural network architectures.

## 4 Experiments

To evaluate the effectiveness of the proposed fKAN, a series of experiments were designed. In the following sections, we provide detailed descriptions of each experiment, covering a range of tasks including deep learning and physics-informed deep learning. The implementation of fKAN and the subsequent experiments are publicly available in the GitHub repository<sup>1</sup>. Additionally, we have created a Python package named `fkan` to simplify using our proposed method.

All experiments were implemented in Python using the latest version of Keras with TensorFlow as the backend for deep learning tasks and PyTorch for physics-informed tasks. The experiments were conducted on a personal computer equipped with an Intel Core-i3 CPU, 16GB of RAM, and an Nvidia 1650 GPU.

### 4.1 Deep learning tasks

In this section, we will conduct several common deep learning tasks to validate the proposed neural block’s effectiveness in handling real-world applications. Specifically, we will assess the accuracy of the proposed fKAN in synthetic regression tasks. Next, we will examine a classification problem in CNNs using the proposed activation function, followed by utilizing a similar CNN network for image denoising tasks. Finally, a one-dimensional CNN (1D-CNN) will be employed for a sentiment analysis task.

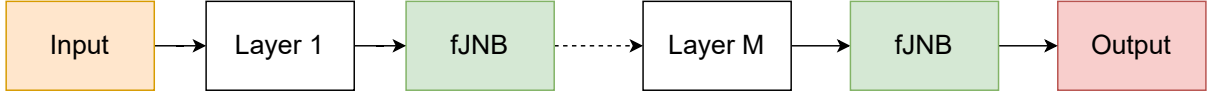
**Regression task** For the first experiment, we consider the following function as the ground truth model:

$$\chi(\zeta) := \sin(\pi\zeta) + 10 \exp\left(\frac{\zeta}{5}\right) + \frac{\epsilon}{100},$$

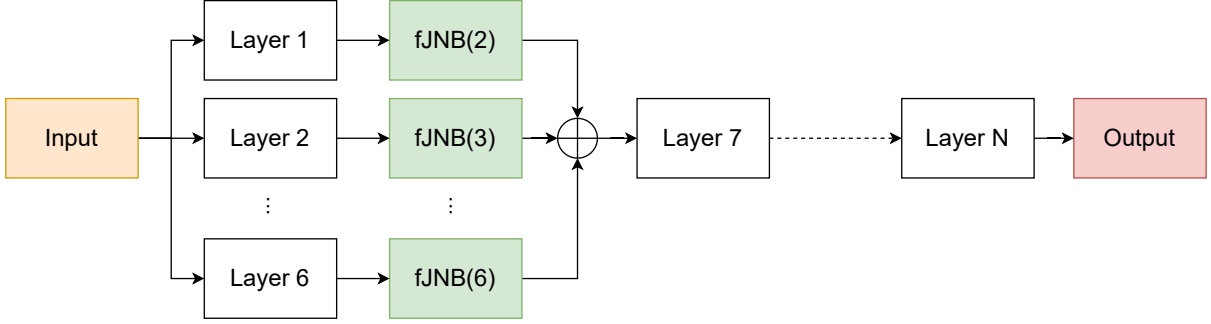
where  $\epsilon$  is standard normal white noise. We sampled 50 equidistant points in the domain  $[-2, 1]$  and split them into train and test sets in a hold-out manner with a test size of 33%. To simulate this problem, we designed a single-layer neural network with varying numbers of neurons. The loss function was set to mean squared error, the optimizer to Adam with a learning rate of 0.01, the maximum iterations to 500, and early stopping with a patience of 200. Figure 4a shows a comparison between the accuracy of the predictions of this network with different activation functions. As can be seen, the proposed fKAN is more accurate than the well-known activation functions as well as a KAN.

For the next validation task, we compare the accuracy of the network for a multi-layer neural network with a fixed number of five neurons in each layer. The hyperparameters of the network are set the same as in the first experiment. The results are shown in Figure 4b and Table 1. Again, it can be seen that the proposed network performs better than the well-known activation functions and alternatives, although there is a higher variance

<sup>1</sup> <https://github.com/alirezaafzalaghaei/fKAN>



(a) Utilizing fJNB in a sequential architecture, where the value of  $q$  may vary for each block. This flexibility allows for the incorporation of different fractional Jacobi basis functions with varying degrees of complexity across successive blocks in the network. By adapting the value of  $q$ , the network can tailor its representation capabilities to better capture the intricacies of the underlying data.



(b) Employing fJNB with varying values of  $q$  concurrently, this deep network comprises six subnetworks, each equipped with distinct fJNBs. By incorporating fJNBs with different  $q$  values, the network can capture a diverse range of features simultaneously. The outputs of these fJNBs are then fused to produce the final prediction, leveraging the collective information gleaned from multiple representations.

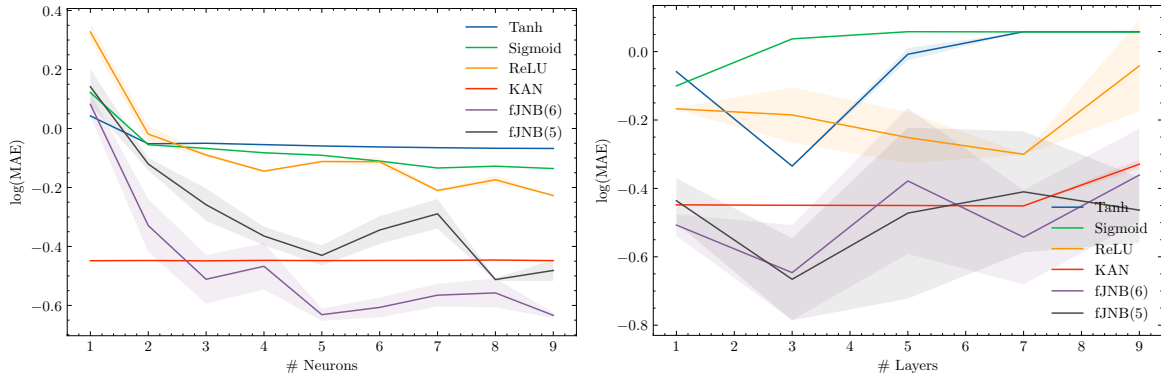
compared to other activation functions. As in the previous example, the KAN has the lowest variance, which can be attributed to its use of a quasi-Newton optimizer in each trial. A notable issue with the KAN is its increased time complexity as the number of layers increases.

To examine the evolution of the Jacobi polynomial parameters ( $\alpha$ ,  $\beta$ , and  $\gamma$ ), we selected a single-layer network with a fixed 5 neurons in the hidden layer, increased the number of samples to 250, and removed the early stopping procedure. Figure 4c depicts the values of these parameters during the training phase. It can be seen that these trainable parameters converge to optimal values in about 250 iterations.

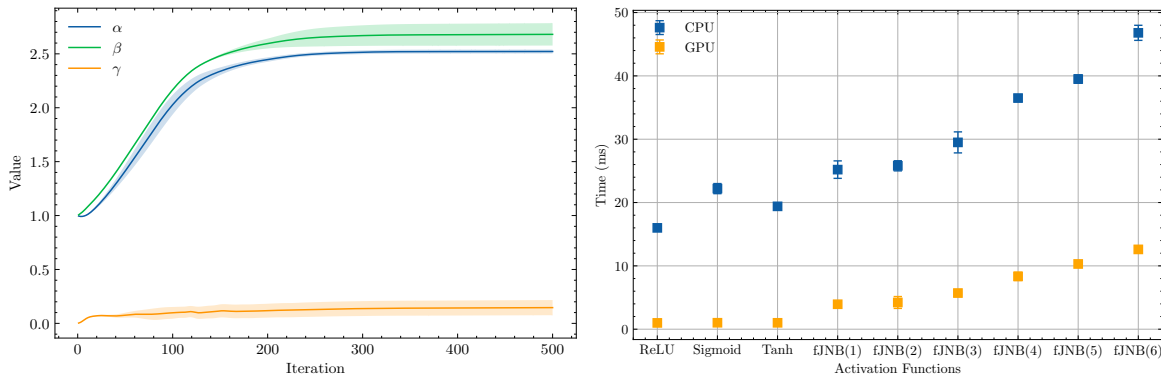
For the last evaluation, we compare the CPU and GPU time needed to compute each activation function. To do this, we generated a random matrix of shape (1000,1000) and evaluated different activation functions. The results are shown in Figure 4d. It can be seen that the proposed activation function in CPU implementation is roughly two times slower than the Sigmoid function and three times slower than the fastest activation function, ReLU.

Act. Func.	No. of hidden layers				
	1	3	5	7	9
SOFTPLUS	0.4390	0.4630	0.4850	0.468	1.7600
SILU	0.6740	0.5190	0.5100	0.337	1.0400
SELU	0.7410	0.9240	0.2290	<b>0.171</b>	0.1270
Leaky ReLU	0.3490	0.2860	0.7060	0.152	0.3540
GELU	0.7130	0.6250	0.7190	0.283	0.1240
ELU	0.6630	0.7520	0.4330	0.786	0.6100
Tanh	0.7940	0.2640	1.2600	1.260	1.2600
Sigmoid	0.7930	1.2400	1.2600	1.260	1.2400
ReLU	0.4290	0.7300	0.3430	0.353	1.7200
JNB(6)	<b>0.0861</b>	<b>0.0186</b>	0.0459	0.177	0.2950
JNB(5)	0.6140	0.6990	<b>0.0168</b>	0.203	<b>0.0218'</b>

Table 1: Comparison of mean absolute error for multi-layer neural networks with different activation functions.



(a) Comparison of prediction accuracy for a single-layer neural network with different activation functions. The proposed activation function demonstrates higher accuracy than well-known functions and KAN. (b) Accuracy comparison for an MLP with a fixed number of neurons per layer. The proposed network performs better than traditional activation functions and alternatives, though with higher variance.



(c) Evolution of Jacobi polynomial parameters ( $\alpha$ ,  $\beta$ , and  $\gamma$ ) during training. The parameters converge to optimal values after approximately 250 iterations. (d) Comparison of CPU and GPU time required to compute various activation functions. The times are the mean of 100 different runs.

Fig. 4: The results of simulation of a one-dimensional function regression task for different activation functions. The proposed activation function demonstrates higher accuracy than well-known functions as well as KAN.

**Image classification** To assess the effectiveness of using generalized Jacobi polynomials as the activation function in fKAN, we utilized the MNIST dataset [45], a well-known benchmark for handwritten digit classification in computer vision and deep learning. The MNIST dataset includes a training set of 60,000 examples and a test set of 10,000 examples, consisting of  $28 \times 28$  grayscale images of digits ranging from zero to nine. For training, we used 54,000 samples and reserved 6,000 samples for validation. The data were normalized to a range between zero and one, then fed into a CNN architecture, illustrated in Figure 5, with a batch size of 512. In this architecture, we varied the activation function to be one of Sigmoid, hyperbolic tangent, ReLU, or fJNB. For each activation function, the network was trained using the Adam optimizer with Keras’s default learning rate over 30 epochs. The accuracy comparisons of these methods are presented in Table 2 and Figure 6. The results indicate that the fractional Jacobi neural block outperforms the alternatives, even within a convolutional deep learning framework.

**Image denoising** For the next experiment, we develop a CNN tailored for image denoising tasks using the Fashion MNIST dataset as our benchmark. This dataset serves as a more complex replacement for the original MNIST data and includes 60,000 samples of  $28 \times 28$  grayscale images categorized into 10 different fashion classes. As with the MNIST data, before feeding the data into the deep model, we scale the values between zero and one.

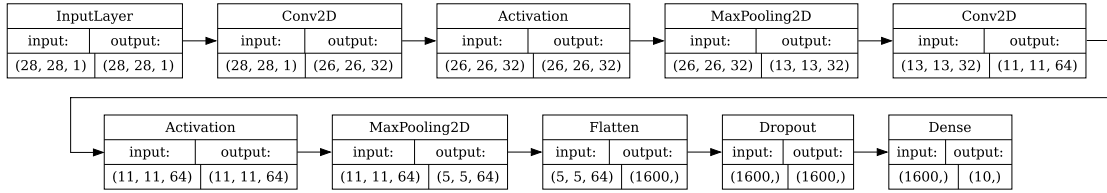


Fig. 5: The architecture of proposed method for MNIST classification data.

Act. Func.	Loss		Accuracy	
	Mean	Std.	Mean	Std.
Sigmoid	0.0611	0.0028	98.092	0.0937
Tanh	0.0322	0.0015	98.904	0.0695
ReLU	0.0256	0.0010	99.140	0.0434
fJNB(2)	0.0252	0.0017	99.134	0.0484
fJNB(3)	0.0224	0.0019	99.200	0.0787
fJNB(4)	<b>0.0217</b>	0.0008	<b>99.228</b>	0.0515
fJNB(5)	0.0249	0.0009	99.204	0.0467
fJNB(6)	0.0290	0.0028	99.024	0.1198

Table 2: Performance of different activation functions in a CNN for classifying MNIST dataset.

The architecture of our CNN for this task is illustrated in Figure 7. We begin by pre-training this CNN with the Fashion MNIST training data. This pre-training step is crucial for enabling the network to learn the underlying structure and distribution of the clean data, thus enhancing its understanding of image features, which is beneficial for the subsequent denoising task. After pre-training, we train the network using pairs of noisy and clean images. Noisy images are generated by adding Gaussian noise with a noise factor of 0.3, serving as input, while the corresponding clean images are used as output. This process teaches the network to effectively map noisy images to their denoised versions. In both the pre-training and denoising training phases, we use a batch size of 512 and train the CNN over 20 epochs using the Adam optimizer with Keras’s default learning rate.

After the training phase, we evaluate the performance of the trained network by comparing the denoising results of the CNN with the ground truth clean images. The results are quantitatively presented in Table 3, which includes PSNR and SSIM metrics to assess the quality of the denoised images. These metrics are defined as:

$$\text{PSNR}(\zeta, \hat{\zeta}) = 10 \log_{10} \left( \frac{\text{MAX}^2\{\zeta\} \cdot MN}{\|\zeta - \hat{\zeta}\|_F^2} \right),$$

where  $\|\cdot\|_F$  is the Frobenius norm,  $\zeta, \hat{\zeta} \in [0, 1]^{M \times N}$ , and

$$\text{SSIM}(\zeta, \hat{\zeta}) = \frac{(2\mu_\zeta\mu_{\hat{\zeta}} + C_1)(2\sigma_{\zeta\hat{\zeta}} + C_2)}{(\mu_\zeta^2 + \mu_{\hat{\zeta}}^2 + C_1)(\sigma_\zeta^2 + \sigma_{\hat{\zeta}}^2 + C_2)},$$

in which  $\mu_\zeta$  and  $\mu_{\hat{\zeta}}$  are the means of  $\zeta$  and  $\hat{\zeta}$ ,  $\sigma_{\zeta\hat{\zeta}}$  is the covariance between  $\zeta$  and  $\hat{\zeta}$ ,  $\sigma_\zeta^2$  and  $\sigma_{\hat{\zeta}}^2$  are the variances of  $\zeta$  and  $\hat{\zeta}$ , respectively. The constants  $C_1$  and  $C_2$  are used to stabilize the division.

**Sentiment Analysis** For the final deep learning experiment, we evaluate the efficiency of the fJNB in a sentiment analysis task using the well-known IMDB dataset, which includes 20,000 samples for training, 5,000 for validation, and 25,000 for testing. The text data is preprocessed using a custom standardization function to remove HTML tags and punctuation. Subsequently, the text is vectorized with a maximum of 20,000 tokens and a sequence length of 500. This processed data is fed into a deep classifier model, which is a 1D CNN comprising

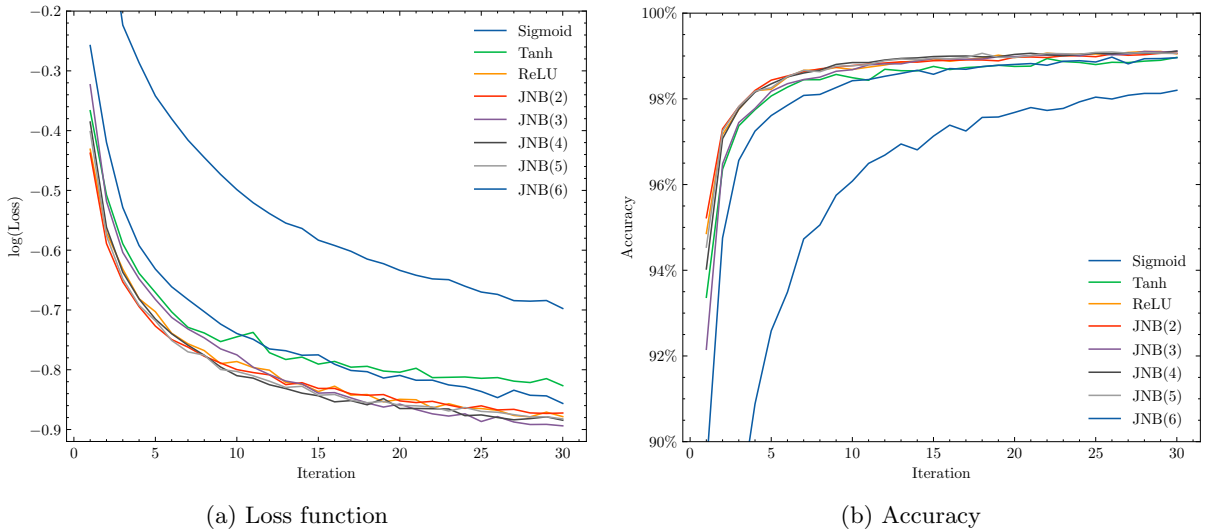


Fig. 6: The loss function and accuracy of the proposed method in comparison to well-known activation functions for classifying the MNIST dataset.

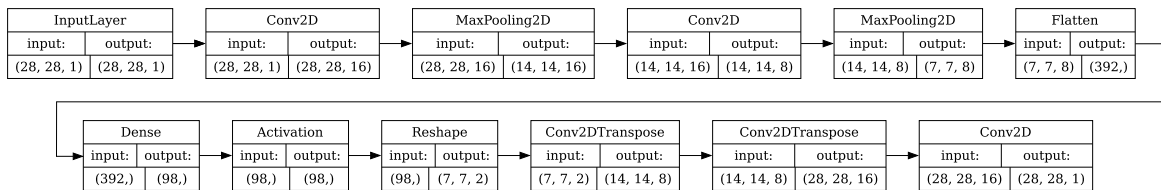


Fig. 7: The architecture of the autoencoder used for denoising Fashion MNIST images. One of the activation functions—Sigmoid, tanh, ReLU, or fJNB with  $q$  values ranging from 2 to 6—is selected to allow for flexible adaptation to different non-linearities in the data.

an embedding layer, dropout layers, convolutional layers, global max pooling, a dense layer, and an output layer. The full architecture is depicted in Figure 8. Similar to the previous examples, we use the Adam optimizer, with a batch size of 512 and 10 epochs for training the network. The performance of the model is evaluated using binary classification metrics, including accuracy, precision, recall, and ROC-AUC, as reported in Table 4.

## 4.2 Physics-informed Deep Learning tasks

To demonstrate the effectiveness of the proposed architecture in solving physical problems, we simulate various types of differential equations within a physics-informed loss function scheme. Mathematically, for a functional operator of the form  $\mathcal{N}(\chi) = \mathcal{S}$ , we define the residual function as  $\mathfrak{R}(\zeta) = \mathcal{N}(\chi)(\zeta) - \mathcal{S}(\zeta)$  and then formulate the loss function of the network as:

$$\text{Loss}(\zeta) = \mathfrak{R}(\zeta)^T \mathfrak{R}(\zeta) + \mathfrak{B}^2 + \mathfrak{J}^2,$$

where  $\mathfrak{B}$  and  $\mathfrak{J}$  represent the network errors for the known boundary and initial conditions, respectively, and  $\zeta \in \mathbb{R}^{N \times d}$  is a vector containing  $N$  training points in the  $d$ -dimensional problem domain. To compute the derivatives of the network with respect to the input parameters, we utilize the standard backpropagation algorithm. For fractional-order derivatives, we employ the Caputo operational matrix of differentiation as proposed by Taheri et al. [84]. This method approximates the fractional derivative using an L1 finite difference scheme in a matrix format, which is then multiplied by the network output to obtain the fractional derivative of the network.

Act, Func.	Pre-train			Denoising		
	MSE	PSNR	SSIM	MSE	PSNR	SSIM
Sigmoid	0.018 ± 0.003	18.026 ± 0.709	0.579 ± 0.043	0.018 ± 0.001	17.813 ± 0.347	0.564 ± 0.019
Tanh	0.017 ± 0.002	18.078 ± 0.545	0.583 ± 0.035	0.018 ± 0.001	17.830 ± 0.261	0.562 ± 0.020
ReLU	0.017 ± 0.001	18.124 ± 0.227	0.577 ± 0.013	0.019 ± 0.001	17.543 ± 0.186	0.537 ± 0.014
fJNB(5)	0.013 ± 0.001	<b>19.205</b> ± 0.300	0.647 ± 0.015	0.017 ± 0.001	18.159 ± 0.308	0.585 ± 0.017
fJNB(6)	<b>0.013</b> ± 0.001	19.171 ± 0.337	<b>0.648</b> ± 0.019	<b>0.016</b> ± 0.001	<b>18.206</b> ± 0.174	<b>0.587</b> ± 0.009

Table 3: Comparison of the accuracy of various activation functions for the Fashion MNIST image denoising task.

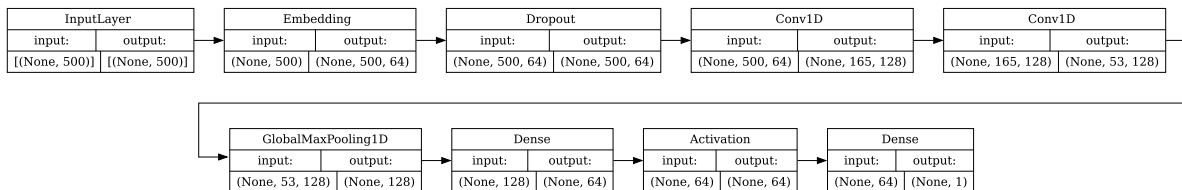


Fig. 8: The architecture of the 1D-CNN used for sentiment analysis on the IMDB dataset. One of the activation functions—Sigmoid, tanh, ReLU, or fJNB with  $q$  values ranging from 1 to 6—is selected to allow for flexible adaptation to different non-linearities in the data.

In the following experiments, we simulate various ordinary, partial, and fractional-order differential equations. Given the complexity of these problems, we utilize the second proposed architecture (Figure 3b), which incorporates multiple fJNBs simultaneously in a network architecture with a concatenation operator. This approach ensures that different polynomial degrees are included in approximating the function.

**Ordinary differential equations** For the first example, we consider the well-known Lane-Emden differential equation in its standard form. This benchmark problem is a second-order singular differential equation given by:

$$\frac{d^2}{d\zeta^2}\chi(\zeta) + \frac{2}{\zeta}\frac{d}{d\zeta}\chi(\zeta) + \chi^m(\zeta) = 0,$$

$$\chi(0) = 1, \quad \chi'(0) = 1,$$

where  $m$  is an integer parameter, typically ranging from zero to five. For this problem, we use 1500 equidistant data points as input. Six fJNB blocks are applied, each to a layer containing 10 neurons. The final layer of the network takes the inputs from 60 different activations of the network and outputs a single real value as the approximation for the Lane-Emden equation. Optimization of this network is performed using the limited memory variant of the quasi-Newton Broyden–Fletcher–Goldfarb–Shanno (L-BFGS) algorithm.

The simulation results for this problem, considering  $m = 0, 1, \dots, 5$ , are depicted in Figure 9. The first root of the predicted function for each value of  $m$  holds physical significance and serves as a criterion for accuracy assessment. Comparison with a similar neural network approach [57] demonstrates significant accuracy improvements (see Table 5).

**Partial differential equations** As a benchmark partial differential equation, we choose the renowned one-dimensional Burgers equation, defined as follows [40]:

$$\frac{\partial}{\partial \tau}\chi(\zeta, \tau) + m_0\chi(\zeta, \tau)\frac{\partial}{\partial \zeta}\chi(\zeta, \tau) - m_1\frac{\partial^2}{\partial \tau^2}\chi(\zeta, \tau) = 0,$$

$$\chi(\zeta, 0) = \frac{m_2}{m_0} + 2\frac{m_1}{m_0}\tanh(x).$$

The exact solution to this problem is given by  $\chi(\zeta, \tau) = \frac{m_2}{m_0} + 2\frac{m_1}{m_0}\tanh(x - m_2\tau)$  for predefined parameters  $m_0, m_1$ , and  $m_2$ . To address this problem, we utilize a neural network with a similar architecture to the previous

Act. Func.	Loss	Accuracy	Precision	Recall	ROC-AUC
Sigmoid	0.604 ± 0.039	85.198 ± 0.468	81.440 ± 1.511	91.266 ± 1.532	91.631 ± 0.422
Tanh	0.610 ± 0.060	85.604 ± 0.818	82.364 ± 2.790	90.912 ± 2.705	91.894 ± 0.505
ReLU	0.808 ± 0.064	83.826 ± 1.141	78.197 ± 2.124	<b>93.995 ± 1.358</b>	91.080 ± 0.404
JNB(1)	0.724 ± 0.074	84.462 ± 1.156	79.967 ± 3.160	92.387 ± 3.090	91.241 ± 0.501
JNB(2)	0.671 ± 0.044	85.205 ± 0.591	80.559 ± 1.374	92.882 ± 1.126	91.306 ± 0.478
JNB(3)	0.646 ± 0.057	84.828 ± 0.761	80.100 ± 1.787	92.808 ± 1.404	91.576 ± 0.416
JNB(4)	<b>0.559 ± 0.062</b>	<b>85.645 ± 0.762</b>	<b>83.395 ± 3.549</b>	89.498 ± 3.916	<b>92.497 ± 0.404</b>
JNB(5)	0.691 ± 0.100	84.247 ± 1.479	79.283 ± 3.401	93.190 ± 2.584	91.454 ± 0.825
JNB(6)	0.627 ± 0.107	84.455 ± 1.658	80.079 ± 4.017	92.371 ± 3.215	91.648 ± 0.985

Table 4: Binary classification metrics for the IMDB dataset using different activation functions.

$m$	Exact	Approximate	Error	GEPINN [57]
0	2.44948974	2.44945454	$3.52 \times 10^{-5}$	$1.40 \times 10^{-7}$
1	3.14159265	3.14160132	$8.67 \times 10^{-6}$	$4.83 \times 10^{-3}$
2	4.35287460	4.35288394	$9.34 \times 10^{-6}$	$8.93 \times 10^{-3}$
3	6.89684860	6.89684915	$5.55 \times 10^{-7}$	$1.88 \times 10^{-2}$
4	14.9715463	14.9712493	$2.97 \times 10^{-4}$	$5.08 \times 10^{-2}$

Table 5: Comparison of the first roots of the predicted solution with the exact roots from [37] and the approximated results from a similar neural network approach [57].

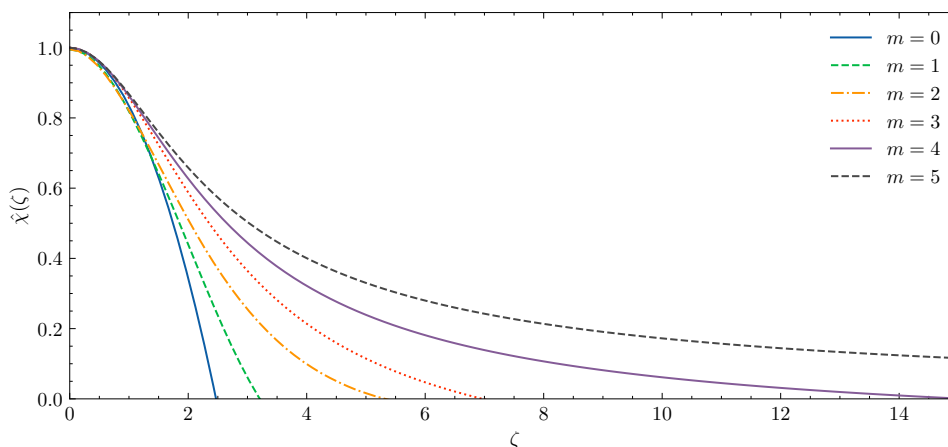


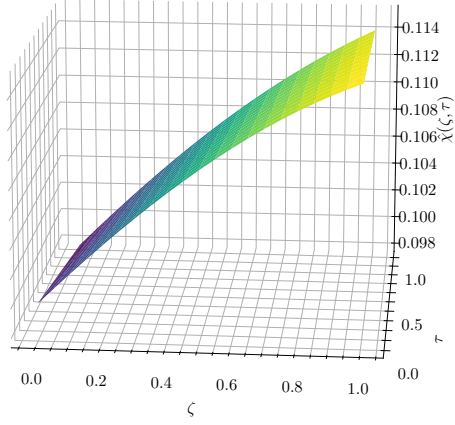
Fig. 9: The simulated results of the Lane-Emden differential equation using the fKAN.

example, with the exception of having two hidden neurons per layer before the fJNB and an input dimension of two to accommodate both time and space variables. For these two variables, we fed the network with a Cartesian product of 100 equidistant points in  $[0, 1]$ . For this example, we compare the predicted solution with the exact solution for two common parameter choices  $m_0, m_1$ , and  $m_2$  as used by Khater et al. [40]. The simulation results are depicted in Figure 10, demonstrating accurate predictions.

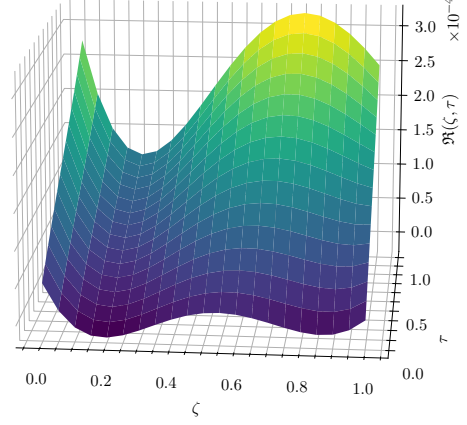
**Fractional differential equations** For the final experiment involving physics-informed neural networks, we investigate a fractional delay differential equation represented as [85]:

$$\frac{d^{0.3}}{d\zeta^{0.3}} \chi(\zeta) = \chi(\zeta - 1) - \chi(\zeta) + 1 - 3\zeta + 3\zeta^2 + \frac{2000\zeta^{2.7}}{1071\Gamma(0.7)},$$

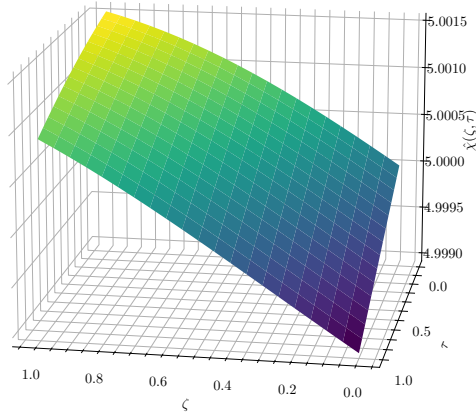
$$\chi(0) = 0,$$



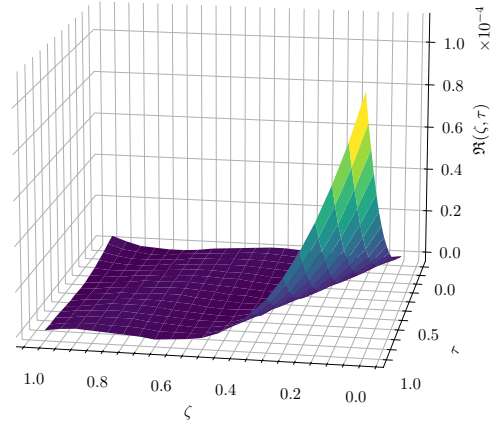
(a) Prediction



(b) Residual



(c) Prediction



(d) Residual

Fig. 10: Simulation results of the Burgers PDE using the fJNB with two sets of parameters:  $m_0, m_1, m_2 = 1, 0.01, 0.1$  (top) and  $m_0, m_1, m_2 = 0.1, 0.0001, 0.5$  (bottom).

where  $\Gamma(\cdot)$  denotes the gamma function and the fractional derivative is defined using the Caputo fractional derivative operator [85, 22]:

$$\frac{d^\alpha}{d\zeta^\alpha} \chi(\zeta) = \frac{1}{\Gamma(1-\alpha)} \int_0^\zeta \frac{\chi'(\tau)}{(\zeta-\tau)^\alpha} d\tau, \quad 0 < \alpha < 1.$$

For simulating this problem, we adopt a similar approach to the previous examples. Specifically, we design the architecture as follows: Each of the first 6 layers connected to fJNBs employs 10 neurons. Subsequently, a concatenation layer is employed. Next, a layer with a weight size of  $60 \times 10$  is used to reduce the network features to 10. Then, three fully connected layers are employed, followed by a final regression neuron. The loss function

is computed using the residual of this equation:

$$\mathfrak{R}(\zeta) = \left[ \mathcal{D}^{0.3} \hat{\chi}(\zeta) \right] - \left[ \hat{\chi}(\zeta - 1) - \hat{\chi}(\zeta) + 1 - 3\zeta + 3\zeta^2 + \frac{2000}{1071\Gamma(0.7)} \zeta^{2.7} \right],$$

where  $\mathcal{D}^\alpha$  is a lower triangular operational matrix of the derivative for the Caputo derivative defined in Taheri et al. [84]. The network weights are then optimized using the L-BFGS algorithm. The predicted solution, the residual with respect to the exact solution, and the network residual loss using this architecture are reported in Figure 11. In this example, we observe fluctuations in the residual errors, which, based on experiments, we found are a direct result of the architectures with multiple fJNBs.

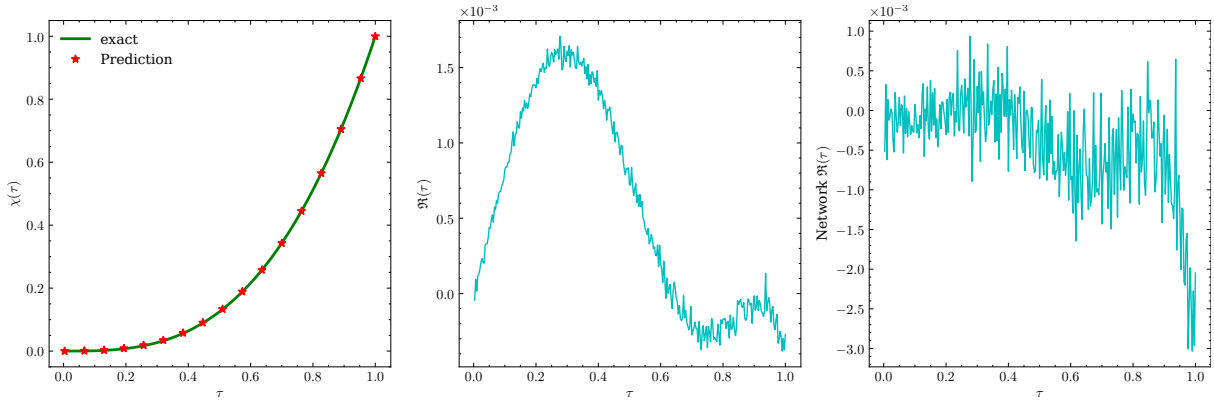


Fig. 11: The simulation results for the fractional delay differential equation using the fJNB architecture.

## 5 Conclusion

This paper introduces a novel extension of the Kolmogorov-Arnold Network framework, incorporating fractional-order orthogonal Jacobi polynomials as basis functions for approximation. Through Equation (1) and Figures 3a and 3b, we demonstrate the integration of this new basis function into the KAN architecture. Comparisons with the Learnable Activation Network [50] highlight the similarities and advantages of our approach.

We observe that the proposed basis function exhibits key characteristics of effective activation functions, including non-linearity, simplicity, and straightforward derivatives. Our study further showcases how the fractional order of these polynomials can be leveraged within neural networks, with parameters adaptively tuned during training.

A comprehensive series of experiments across various deep learning tasks, including MLP and 1D/2D-CNN architectures, underscores the superior performance of the fractional KAN over traditional KAN and other activation functions. However, we acknowledge limitations such as increased time complexity compared to simpler activation functions and reduced interpretability relative to KAN due to the global nature of the basis functions. Future work may explore local basis function variants, like fractional B-splines, to address these limitations.

## References

- [1] Diab W Abueidda, Panos Pantidis, and Mostafa E Mobasher. “Deepokan: Deep operator network based on kolmogorov arnold networks for mechanics problems”. In: *arXiv preprint arXiv:2405.19143* (2024).
- [2] Charu C Aggarwal et al. “Neural networks and deep learning”. In: *Springer* 10.978 (2018), p. 3.
- [3] Fawaz E Alsaadi et al. “Control of a Hydraulic Generator Regulating System Using Chebyshev-Neural-Network-Based Non-Singular Fast Terminal Sliding Mode Method”. In: *Mathematics* 11.1 (2023), p. 168.

- [4] Emad M Alsaedi et al. “Classification of Encrypted Data Using Deep Learning and Legendre Polynomials”. In: *The International Conference on Innovations in Computing Research*. Springer. 2022, pp. 331–345.
- [5] Martin Arjovsky, Amar Shah, and Yoshua Bengio. “Unitary evolution recurrent neural networks”. In: *International conference on machine learning*. PMLR. 2016, pp. 1120–1128.
- [6] J Arvesú, K Driver, and LL Littlejohn. “Zeros of Jacobi and ultraspherical polynomials”. In: *The Ramanujan Journal* (2021), pp. 1–20.
- [7] S Benzoubeir, A Hmamed, and H Qjidaa. “Hypergeometric Laguerre moment for handwritten digit recognition”. In: *2009 International Conference on Multimedia Computing and Systems*. IEEE. 2009, pp. 449–453.
- [8] Johan Bjorck et al. *Understanding Batch Normalization*. 2018. arXiv: 1806.02375 [cs.LG].
- [9] Thierry Blu and Michael Unser. “The fractional spline wavelet transform: definition and implementation”. In: *2000 IEEE International Conference on Acoustics, Speech, and Signal Processing. Proceedings (Cat. No. 00CH37100)*. Vol. 1. IEEE. 2000, pp. 512–515.
- [10] YEVGENIY BODYANSKIY and SERHII KOSTIUK. “Learnable Extended Activation Function for Deep Neural Networks”. In: *International Journal of Computing (Oct. 2023)* (2023), pp. 311–318.
- [11] Zavareh Bozorgasl and Hao Chen. “Wav-kan: Wavelet kolmogorov-arnold networks”. In: *arXiv preprint arXiv:2405.12832* (2024).
- [12] Jürgen Braun and Michael Griebel. “On a constructive proof of Kolmogorov’s superposition theorem”. In: *Constructive approximation* 30 (2009), pp. 653–675.
- [13] BC Carlson. “B-splines, hypergeometric functions, and Dirichlet averages”. In: *Journal of approximation theory* 67.3 (1991), pp. 311–325.
- [14] Yinghao Chen et al. “Numerical solving of the generalized Black-Scholes differential equation using Laguerre neural network”. In: *Digital Signal Processing* 112 (2021), p. 103003.
- [15] Minjong Cheon. “Kolmogorov-Arnold Network for Satellite Image Classification in Remote Sensing”. In: *arXiv preprint arXiv:2406.00600* (2024).
- [16] Djork-Arné Clevert, Thomas Unterthiner, and Sepp Hochreiter. “Fast and accurate deep network learning by exponential linear units (elus)”. In: *arXiv preprint arXiv:1511.07289* (2015).
- [17] M Deepthi, GNVR Vikram, and P Venkatappareddy. “Development of a novel activation function based on Chebyshev polynomials: an aid for classification and denoising of images”. In: *The Journal of Supercomputing* (2023), pp. 1–17.
- [18] Mehdi Delkosh and Kouros Parand. “A new computational method based on fractional Lagrange functions to solve multi-term fractional differential equations”. In: *Numerical Algorithms* (), pp. 1–38.
- [19] Sergio A Dorado-Rojas, Bhanukiran Vinzamuri, and Luigi Vanfretti. “Orthogonal laguerre recurrent neural networks”. In: *Mach. Learn. and the Phys. Sci. Workshop at the 34th Conf. on Neural Info. Proc. Syst.(NeurIPS)*. 2020.
- [20] S Dzhenezher and A Skopenkov. “A structured proof of Kolmogorov’s Superposition Theorem”. In: *arXiv preprint arXiv:2105.00408* (2021).
- [21] A Ebrahimzadeh, M Ahmadi, and M Safarnejad. “Classification of ECG signals using Hermite functions and MLP neural networks”. In: *Journal of AI and Data Mining* 4.1 (2016), pp. 55–65.
- [22] Ali Nosrati Firoozsalari et al. “deepFDNet: A novel neural network architecture for solving fractional differential equations”. In: *arXiv preprint arXiv:2309.07684* (2023).
- [23] Brigitte Forster and Peter Massopust. “Splines of complex order: Fourier, filters and fractional derivatives”. In: *Sampling Theory in Signal and Image Processing* 10.1 (2011), pp. 89–109.
- [24] Christian Garbin, Xingquan Zhu, and Oge Marques. “Dropout vs. batch normalization: an empirical study of their impact to deep learning”. In: *Multimedia tools and applications* 79.19 (2020), pp. 12777–12815.
- [25] Walter Gautschi. *Orthogonal polynomials: computation and approximation*. OUP Oxford, 2004.
- [26] Remi Genet and Hugo Inzirillo. “A Temporal Kolmogorov-Arnold Transformer for Time Series Forecasting”. In: *arXiv preprint arXiv:2406.02486* (2024).

- [27] Remi Genet and Hugo Inzirillo. “Tkan: Temporal kolmogorov-arnold networks”. In: *arXiv preprint arXiv:2405.07344* (2024).
- [28] Federico Girosi and Tomaso Poggio. “Representation properties of networks: Kolmogorov’s theorem is irrelevant”. In: *Neural Computation* 1.4 (1989), pp. 465–469.
- [29] Xavier Glorot, Antoine Bordes, and Yoshua Bengio. “Deep sparse rectifier neural networks”. In: *Proceedings of the fourteenth international conference on artificial intelligence and statistics*. JMLR Workshop and Conference Proceedings. 2011, pp. 315–323.
- [30] Gustaf Gripenberg. “Approximation by neural networks with a bounded number of nodes at each level”. In: *Journal of approximation theory* 122.2 (2003), pp. 260–266.
- [31] Yuhe Guo and Zhewei Wei. “Graph Neural Networks with Learnable and Optimal Polynomial Bases”. In: *arXiv preprint arXiv:2302.12432* (2023).
- [32] Amir Hosein Hadian Rasanan et al. “Simulation of nonlinear fractional dynamics arising in the modeling of cognitive decision making using a new fractional neural network”. In: *Mathematical Methods in the Applied Sciences* 43.3 (2020), pp. 1437–1466.
- [33] Zeinab Hajimohammadi et al. “Fractional Chebyshev deep neural network (FCDNN) for solving differential models”. In: *Chaos, Solitons & Fractals* 153 (2021), p. 111530.
- [34] Jun Han and Claudio Moraga. “The influence of the sigmoid function parameters on the speed of backpropagation learning”. In: *From Natural to Artificial Neural Computation: International Workshop on Artificial Neural Networks Malaga-Torremolinos, Spain, June 7–9, 1995 Proceedings 3*. Springer. 1995, pp. 195–201.
- [35] Kaiming He et al. “Delving deep into rectifiers: Surpassing human-level performance on imagenet classification”. In: *Proceedings of the IEEE international conference on computer vision*. 2015, pp. 1026–1034.
- [36] Dan Hendrycks and Kevin Gimpel. “Gaussian error linear units (gelus)”. In: *arXiv preprint arXiv:1606.08415* (2016).
- [37] George Paul Horedt. *Polytropes: applications in astrophysics and related fields*. Vol. 306. Springer Science & Business Media, 2004.
- [38] Sergey Ioffe and Christian Szegedy. “Batch normalization: Accelerating deep network training by reducing internal covariate shift”. In: *International conference on machine learning*. pmlr. 2015, pp. 448–456.
- [39] Ameya Jagtap and George Em Karniadakis. “How important are activation functions in regression and classification? A survey, performance comparison, and future directions”. In: *Journal of Machine Learning for Modeling and Computing* (2022).
- [40] AH Khater, RS Temsah, and MM2474624 Hassan. “A Chebyshev spectral collocation method for solving Burgers’-type equations”. In: *Journal of computational and applied mathematics* 222.2 (2008), pp. 333–350.
- [41] Patrick Kidger and Terry Lyons. “Universal approximation with deep narrow networks”. In: *Conference on learning theory*. PMLR. 2020, pp. 2306–2327.
- [42] Andrei Nikolaevich Kolmogorov. “On the representation of continuous functions of many variables by superposition of continuous functions of one variable and addition”. In: *Doklady Akademii Nauk*. Vol. 114. 5. Russian Academy of Sciences. 1957, pp. 953–956.
- [43] Wataru Kumagai and Akiyoshi Sannai. “Universal approximation theorem for equivariant maps by group cnns”. In: *arXiv preprint arXiv:2012.13882* (2020).
- [44] Susanna Lange, Kyle Helfrich, and Qiang Ye. *Batch Normalization Preconditioning for Neural Network Training*. 2022. arXiv: 2108.01110 [cs.LG].
- [45] Yann LeCun. “The MNIST database of handwritten digits”. In: <http://yann.lecun.com/exdb/mnist/> (1998).
- [46] Yann LeCun et al. “Efficient backprop”. In: *Neural networks: Tricks of the trade*. Springer, 2002, pp. 9–50.
- [47] Ziyao Li. “Kolmogorov-Arnold Networks are Radial Basis Function Networks”. In: *arXiv preprint arXiv:2405.06721* (2024).

- [48] Hongliang Liu et al. “Jacobi Neural Network Method for Solving Linear Differential-Algebraic Equations with Variable Coefficients”. In: *Neural Processing Letters* 53.5 (2021), pp. 3357–3374.
- [49] Mengxi Liu et al. “iKAN: Global Incremental Learning with KAN for Human Activity Recognition Across Heterogeneous Datasets”. In: *arXiv preprint arXiv:2406.01646* (2024).
- [50] Ziming Liu et al. “Kan: Kolmogorov-arnold networks”. In: *arXiv preprint arXiv:2404.19756* (2024).
- [51] GG Lorentz. “Metric entropy, widths, and superpositions of functions”. In: *The American Mathematical Monthly* 69.6 (1962), pp. 469–485.
- [52] Zhou Lu et al. “The expressive power of neural networks: A view from the width”. In: *Advances in neural information processing systems* 30 (2017).
- [53] Liying Ma and Khashayar Khorasani. “Constructive feedforward neural networks using Hermite polynomial activation functions”. In: *IEEE Transactions on Neural Networks* 16.4 (2005), pp. 821–833.
- [54] Andrew L Maas, Awni Y Hannun, Andrew Y Ng, et al. “Rectifier nonlinearities improve neural network acoustic models”. In: *Proc. icml*. Vol. 30. 1. Atlanta, Georgia, USA. 2013, p. 3.
- [55] Susmita Mall and Snehashish Chakraverty. “Application of Legendre neural network for solving ordinary differential equations”. In: *Applied Soft Computing* 43 (2016), pp. 347–356.
- [56] Carla Manni, Fabio Roman, and Hendrik Speleers. “Generalized B-splines in isogeometric analysis”. In: *Approximation Theory XV: San Antonio 2016 15*. Springer. 2017, pp. 239–267.
- [57] Hassan Dana Mazraeh and Kouros Parand. “GEPINN: An innovative hybrid method for a symbolic solution to the Lane-Emden type equation based on grammatical evolution and physics-informed neural networks”. In: *Astronomy and Computing* (2024), p. 100846.
- [58] Diganta Misra. “Mish: A self regularized non-monotonic activation function”. In: *arXiv preprint arXiv:1908.08681* (2019).
- [59] Vinod Nair and Geoffrey E Hinton. “Rectified linear units improve restricted boltzmann machines”. In: *Proceedings of the 27th international conference on machine learning (ICML-10)*. 2010, pp. 807–814.
- [60] Takato Nishijima. “Universal approximation theorem for neural networks”. In: *arXiv preprint arXiv:2102.10993* (2021).
- [61] K Parand, H Yousefi, and M Delkhosh. “A numerical approach to solve Lane-Emden type equations by the fractional order of rational Bernoulli functions”. In: *Romanian J. Phys* 62.104 (2017), pp. 1–24.
- [62] Kouros Parand and Mehdi Delkhosh. “Accurate solution of the Thomas–Fermi equation using the fractional order of rational Chebyshev functions”. In: *Journal of Computational and Applied Mathematics* 317 (2017), pp. 624–642.
- [63] Kouros Parand and Mehdi Delkhosh. “Solving Volterra’s population growth model of arbitrary order using the generalized fractional order of the Chebyshev functions”. In: *Ricerche di Matematica* 65 (2016), pp. 307–328.
- [64] Kouros Parand et al. “Fractional order of rational Jacobi functions for solving the non-linear singular Thomas-Fermi equation”. In: *The European Physical Journal Plus* 132 (2017), pp. 1–13.
- [65] Kouros Parand et al. “Parallel LS-SVM for the numerical simulation of fractional Volterra’s population model”. In: *Alexandria Engineering Journal* 60.6 (2021), pp. 5637–5647.
- [66] Jagdish Chandra Patra, Pramod Kumar Meher, and Goutam Chakraborty. “Development of Laguerre neural-network-based intelligent sensors for wireless sensor networks”. In: *IEEE Transactions on instrumentation and measurement* 60.3 (2010), pp. 725–734.
- [67] Ashis Paul et al. “SinLU: Sinu-sigmoidal linear unit”. In: *Mathematics* 10.3 (2022), p. 337.
- [68] Leif E Peterson and Kirill V Larin. “Image classification of artificial fingerprints using Gabor wavelet filters, self-organising maps and Hermite/Laguerre neural networks”. In: *International Journal of Knowledge Engineering and Soft Data Paradigms* 1.3 (2009), pp. 239–256.
- [69] Allan Pinkus. “Approximation theory of the MLP model in neural networks”. In: *Acta numerica* 8 (1999), pp. 143–195.
- [70] Evgenii Pishchik. “Trainable Activations for Image Classification”. In: (2023).

- [71] Francesca Pitolli. “A fractional B-spline collocation method for the numerical solution of fractional predator-prey models”. In: *Fractal and Fractional* 2.1 (2018), p. 13.
- [72] Yi Qin, Xin Wang, and Jingqiang Zou. “The optimized deep belief networks with improved logistic sigmoid units and their application in fault diagnosis for planetary gearboxes of wind turbines”. In: *IEEE Transactions on Industrial Electronics* 66.5 (2018), pp. 3814–3824.
- [73] Jamal Amani Rad, Kouros Parand, and Snehashish Chakraverty. *Learning with fractional orthogonal kernel classifiers in support vector machines: Theory, algorithms and applications*. Springer, 2023.
- [74] Prajit Ramachandran, Barret Zoph, and Quoc V Le. “Searching for activation functions”. In: *arXiv preprint arXiv:1710.05941* (2017).
- [75] Gerasimos G Rigatos and Spyros G Tzafestas. “Feed-forward neural networks using Hermite polynomial activation functions”. In: *Advances in Artificial Intelligence: 4th Hellenic Conference on AI, SETN 2006, Heraklion, Crete, Greece, May 18-20, 2006. Proceedings 4*. Springer, 2006, pp. 323–333.
- [76] Moein E Samadi, Younes Müller, and Andreas Schuppert. “Smooth Kolmogorov Arnold networks enabling structural knowledge representation”. In: *arXiv preprint arXiv:2405.11318* (2024).
- [77] Johannes Schmidt-Hieber. “The Kolmogorov–Arnold representation theorem revisited”. In: *Neural networks* 137 (2021), pp. 119–126.
- [78] Wolfgang Schweizer. “Orthogonal Polynomials: General Aspects”. In: *Special Functions in Physics with MATLAB*. Cham: Springer International Publishing, 2021, pp. 181–197. ISBN: 978-3-030-64232-7. DOI: 10.1007/978-3-030-64232-7\_15. URL: [https://doi.org/10.1007/978-3-030-64232-7\\_15](https://doi.org/10.1007/978-3-030-64232-7_15).
- [79] Jie Shen, Tao Tang, and Li-Lian Wang. *Spectral methods: algorithms, analysis and applications*. Vol. 41. Springer Science & Business Media, 2011.
- [80] Sankatha Prasad Singh, JHW Burry, and B Watson. *Approximation theory and spline functions*. Vol. 136. Springer Science & Business Media, 2012.
- [81] David A Sprecher. “On the structure of continuous functions of several variables”. In: *Transactions of the American Mathematical Society* 115 (1965), pp. 340–355.
- [82] Sidharth SS. “Chebyshev Polynomial-Based Kolmogorov–Arnold Networks: An Efficient Architecture for Nonlinear Function Approximation”. In: *arXiv preprint arXiv:2405.07200* (2024).
- [83] SynodicMonth. *ChebyKAN*. <https://github.com/SynodicMonth/ChebyKAN>. 2024.
- [84] Tayebah Taheri, Alireza Afzal Aghaei, and Kouros Parand. “Accelerating Fractional PINNs using Operational Matrices of Derivative”. In: *arXiv preprint arXiv:2401.14081* (2024).
- [85] Tayebah Taheri, Alireza Afzal Aghaei, and Kouros Parand. “Bridging machine learning and weighted residual methods for delay differential equations of fractional order”. In: *Applied Soft Computing* 149 (2023), p. 110936.
- [86] Qian Tao et al. “LONGNN: Spectral GNNs with Learnable Orthonormal Basis”. In: *arXiv preprint arXiv:2303.13750* (2023).
- [87] Michael Unser and Thierry Blu. “Fractional splines and wavelets”. In: *SIAM review* 42.1 (2000), pp. 43–67.
- [88] P Venkatappareddy et al. “A Legendre polynomial based activation function: An aid for modeling of max pooling”. In: *Digital Signal Processing* 115 (2021), p. 103093.
- [89] Nelson Vieira. “Bicomplex Neural Networks with Hypergeometric Activation Functions”. In: *Advances in Applied Clifford Algebras* 33.2 (2023), p. 20.
- [90] Cong Wang, Hongli Zhang, and Ping Ma. “Wind power forecasting based on singular spectrum analysis and a new hybrid Laguerre neural network”. In: *Applied Energy* 259 (2020), p. 114139.
- [91] Xiyuan Wang and Muhan Zhang. “How powerful are spectral graph neural networks”. In: *International Conference on Machine Learning*. PMLR, 2022, pp. 23341–23362.
- [92] Jinfeng Xu et al. “FourierKAN-GCF: Fourier Kolmogorov–Arnold Network—An Effective and Efficient Feature Transformation for Graph Collaborative Filtering”. In: *arXiv preprint arXiv:2406.01034* (2024).